Comparative performance assessment of four BIPV roof solutions in the Netherlands

Comparative performance assessment of four BIPV roof solutions in the Netherlands

M.J. Ritzen[1,2], Z.A.E.P Vroon[1,3], R. Rovers[1], C.P.W. Geurts[2,3]

[1] RiBuilT / Zuyd University of Applied Sciences, Heerlen, the Netherlands
[2] Eindhoven University of Technology, Department of the Built Environment, Eindhoven, the Netherlands
[3] TNO, Delft/Eindhoven, the Netherlands
Corresponding author: Michiel Ritzen, michiel.ritzen@zuyd.nl

Abstract

A significant amount of global energy consumption takes place in the built environment, with as collateral effect CO_2-related climate change. One of the strategies to realize a significant CO_2 reduction is by integrating photovoltaic modules in the building envelope (BIPV). Disadvantages of BIPV include a possibly lower energy output and a possibly decreased life span due to the lack of optimal cooling of the PV modules. Currently, cooling of PV modules is usually realized by passive back-string ventilation, which is under strain when integration PV modules in the building envelope. In this study, a comparative field study of BIPV is conducted in the field lab 'The District of Tomorrow' to generate insight into BIPV efficiency as a function of back-string ventilation. This paper presents a selection of the monitoring results of the realized system, consisting of 24 PV modules in 4 segments with a total of 6000 Wp output with different amounts of back-string ventilation. The measurements indicate that in a moderate climate BIPV solutions without back-string ventilation result in increased operating temperatures, lower electricity output and condensation between PV modules and rooftop surface. To decrease relative humidity levels and operating temperatures to acceptable values, back-string ventilation is seen as an effective cooling medium in the presented field case.

1 Introduction

Between 1990 and 2005, global final energy consumption increased by 23%, while the associated CO2 emissions increased by 25% [1]. This consumption is expected to grow by another 45% between 2002 and 2025 [2]. Of this global energy consumption 20% to 40% is consumed in the built environment [3], of which more than 86% is based on fossil fuels [4]. Between 1995 and 2005, extraction of fossil fuels increased by 24% [5]. To lower overall energy consumption in the built environment and to lower dependency on fossil fuels, it has been agreed within the EU that all new buildings in 2020 have to be (nearly) zero-energy buildings (NZEB) [3, 6]. NZEB implies that all building related operating energy is generated on the building site itself by using renewable sources, calculated on a yearly basis [7, 8].

The building envelope plays a significant role in energy performance [9], as it provides the necessary space for the installation of active solar energy systems for energy generation [10] and influences the energy gains/losses through insulation values of opaque and transparent components.

One of the solutions to provide the necessary energy in the building itself is by applying active solar energy-generating devices in the form of photovoltaic (PV) modules for electricity. In a PV system solar radiation is converted into electricity, which can be used in the building itself or can be fed into the electricity grid. As the energy received from the sun on the earth's surface in one hour is equal to approximately one year's energy needs for mankind [11, 12], we have the ability to fulfil our

energy needs completely using the sun, even with the current efficiency of PV systems of between 12% and 19%.

PV systems can be added to a building (Building Applied PV - BAPV) or can be integrated in the building envelope (Building Integrated PV – BIPV), as illustrated by Fig. 1. and Fig. 2. BIPV is part of the building design, possibly replacing conventional building materials such as wall cladding and /or roofing. To realize buildings of which the operational energy is fully generated by PV modules, integrating these modules in the building envelope will lead to aesthetically acceptable solutions and contribute to large-scale realization of NZEBs. BIPV solutions generally result in a decrease of space between the PV installation and the thermal building envelope, negatively affecting the natural back-string ventilation.

Fig. 1. and 2. Examples of two projects with Building Applied PV (BAPV) and Building Integrated PV (BIPV) in the Netherlands.

Back-string ventilation is one of the methods to effectively cool PV systems [13-23] and is one of the aspects that is under constraint when integrating the energy-generating devices in the building envelope. This has a negative effect on PV performance because the efficiency of PV crystalline silicon cells drops by approximately 0.5% per K temperature rise [24, 25]. Besides that, higher temperatures of the PV modules might lead to a shortened lifespan and lack of ventilation might lead to condensation in the structure.

In this study, the effect of PV integration in the building envelope regarding PV system performance is investigated. Four segments, with a total of 6000 WP, with different amounts of back-string ventilation were extensively monitored in a field test in The District of Tomorrow (Fig. 3.). The difference in back-string ventilation was realized by installing the mechanical ventilation outlet behind two segments (Fig. 4.). One segment was left as-is with natural ventilation, and the air gap behind one segment was sealed, as indicated in Fig. 5. A further description of the installation is given in Section 2.1. The monitoring installation consisted of temperature sensors, air-velocity sensors, relative humidity sensors, a wind direction sensor and a pyranometer. A further description of the monitoring installation is given in Section 2.2.

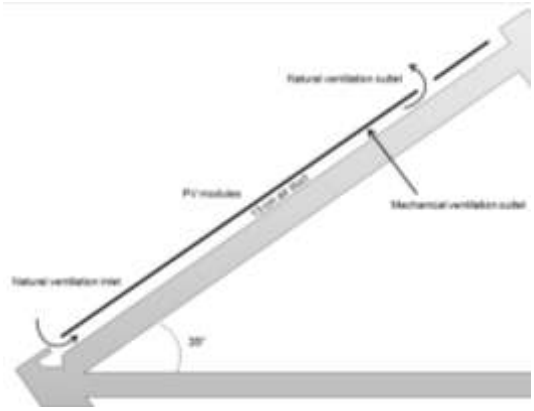

Fig. 3. and 4. PV field test in The District of Tomorrow consisting of 4 segments of PV modules and a vertical section of the field test with ventilation in and outlets providing different amounts of back-string ventilation.

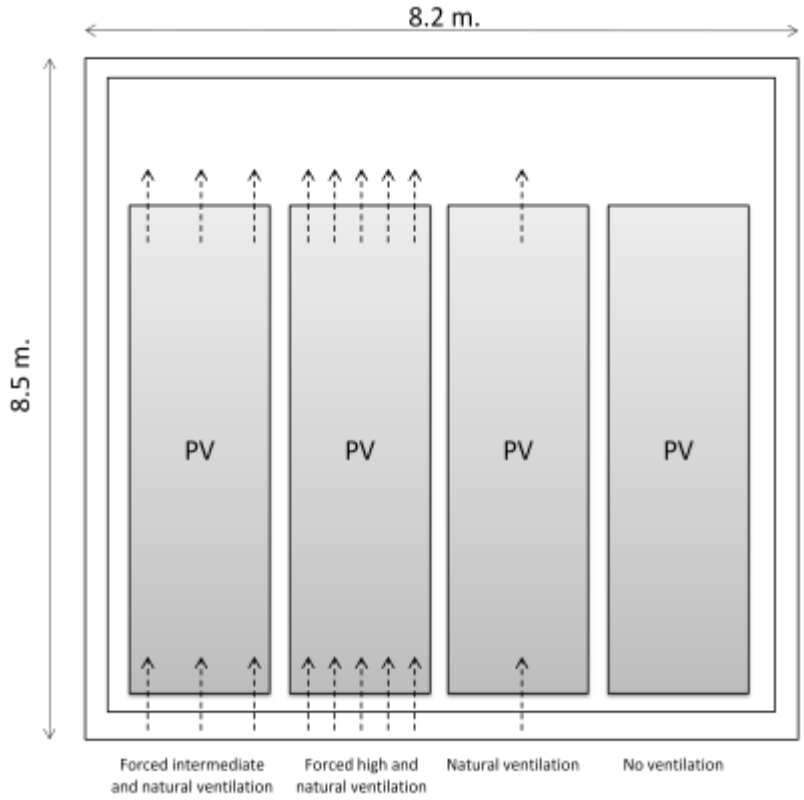

Fig. 5. Rooftop overview of the four PV segments with different amounts of back-string ventilation in the PV field test in The District of Tomorrow.

Similar research and tests have been conducted on a smaller scale [19, 22, 23, 26] and similar sized arrays have been monitored, but without fluctuating the back-string ventilation [27-30]. Moreover, combinations of Building Integrated PV (BIPV) with other functions in the building envelope are being studied, but without the fluctuation of ventilation [10, 16, 31-36].

2 Field test site

The location of the field test in the District of Tomorrow (TDoT), Heerlen, the Netherlands, has a moderate sea climate (type Cfb according to Köppen)) with relatively mild summers (17.5°C), mild winters (3.1°C) and annually 773 mm of precipitation [37]. The exact geographic location is 50°49'47.48" latitude, 6°1'2.06" longitude and 183 m. altitude. The location is an open site without major disturbance from building objects. The highway between Heerlen and Aachen (Germany) is southwest of the location. In TDoT 4 experimental building objects are being realized with amongst other elements innovative PV solutions. The field test in this study is part of building 1, indicated in Fig. 6.

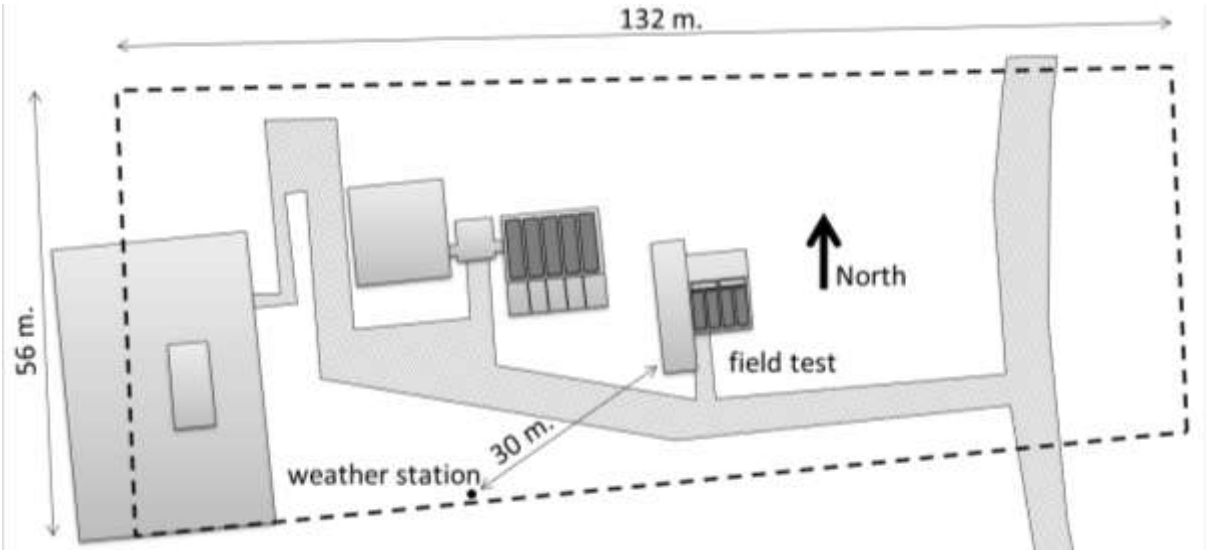

Fig. 6. Plan of The District of Tomorrow with the weather station installed approx. 30 m. west to southwest of the field test.

2.1 PV installation

The PV components of the field test have the following specifications:

a) Orientation 190° (SSW)
b) Inclination 35°
c) frames (6.0 x 1.68 m)
d) 6 modules 1x1.6 m per frame, type Solland Solar
e) 60 mono-crystalline cells per module, type Sunweb®
f) segments (6000 Wp with 1440 cells)
g) inverters type SMA sunnyboy 1200 (1 per string / frame)
h) Efficiency 16% (indicated by manufacturer)
i) Location: open field

2.2 Monitoring installation

The design, realization and monitoring of the system accords with the international standard IEC 1829 (Chrystalline silicon photovoltaic (PV) array – on-site measurement of I-V characteristics) [38] and the international standard IEC 61724 (Photovoltaic system performance monitoring – guidelines for measurement, data exchange and analysis) [27]. Figure 7 shows an overview of measurements in the field test.

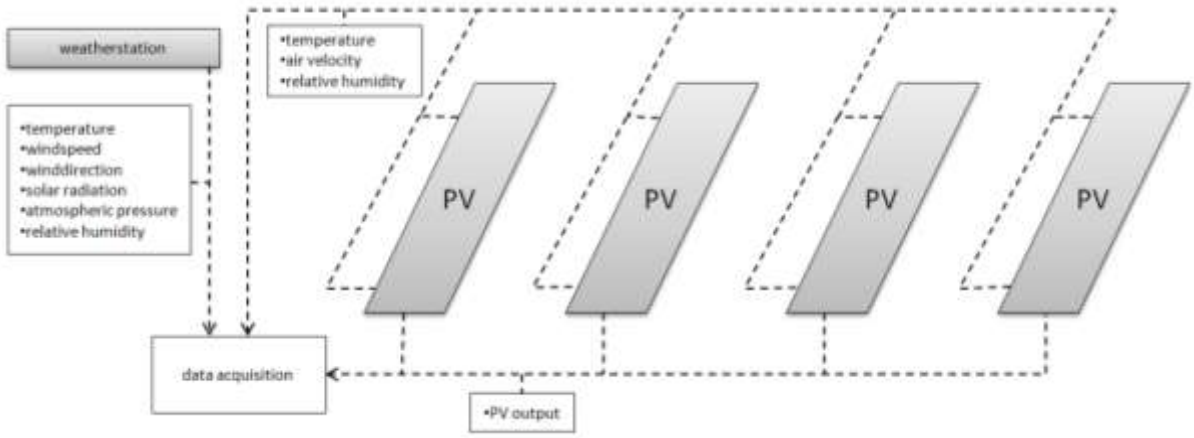

Fig. 7. Overview of measurements in the field test consisting of sensors on the PV installation, a weather station and PV output.

The monitoring installation consists of the following:

a) A weather station, type Delta Ohm HD52.3D 147R, is installed at a height of approximately 191 m. above sea level, 8 m above local level, located approximately 30 m. west to south-west of the field test. (Fig. 6), consisting of the components indicated in Table 1.
b) 16 PT100 4-wire surface temperature sensors, type Delta Ohm TP878.1SS, placed in the centre on the back of the PV modules at the top and bottom of the segments, and placed on the rooftop directly opposite the sensors on the PV modules (see Fig. 8, 9, 10, and 11). Range + 4°C - + 85°C. Indicated by 'PTxx' in Fig. 8 and 9.
c) 6 air-temperature, air-velocity and relative humidity sensors, type Delta Ohm HD29.371, placed in the air gap between the PV modules and the rooftop. Temperature range: -10 ^{0}C - +60^{0}C; accurancy: +/- 0.3^{0}C. Air-velocity range: 0.05 - 1 m/s, accuracy +/- 0.06 m/s + 2% of measurement at 50 % RH and 1013 hPa. Relative humidity range 5-98% RH, accuracy +/-2.5% (5-90%RH) - +/- 3.5% remaining range. Indicated by 'TVLxx' in Fig. 8 and 9.
d) 3 air-temperature and air-velocity sensors, type Delta Ohm HD29.37, placed in the outlets of the mechanical ventilation between the PV modules and the rooftop. Temperature range: -10 ^{0}C - +60^{0}C; accurancy: +/- 0.3^{0}C. Air-velocity range: 0.05 - 1 m/s, accuracy +/- 0.06 m/s + 2% of measurement at 50 % RH and 1013 hPa.
e) 2 air-temperature and relative humidity sensors, type Delta Ohm HD4817TC1.2, placed in the air-gap between the PV modules and the rooftop. Temperature range -20 ^{0}C - +80^{0}C, accuracy +/-0.3^{0}C (0- +70 ^{0}C), +/-0.4^{0}C (-10 ^{0}C - 0^{0}C and +70 ^{0}C - +80^{0}C). Relative humidity range 0-100%RH, accuracy +/-2% (10-90%RH), +/-2.5% outside. Indicated by 'TLxx' in Fig. 8 and 9.
f) 4 air-pressure-difference sensors, type Delta Ohm HD408T-20MBD, placed in the air gap between the PV modules and the rooftop to indicate the direction of airflow per segment.
g) 1 SMA sunny webbox for monitoring PV output per segment and in total. The webbox generates data output with a 5-minute resolution based on measurements every 1 second. Generated data consists of operating time (h), output (W), output (kWh), frequency (Hz), isolation (kOhm), voltage (V), ampere (A), and operating status. PV output per segment is measured after the inverter. Decreasing efficiency of the inverters might be of influence on the measurements.

Table 1. Specifications of the components of the weather station in The District of Tomorrow (TDoT).

Component	Method	Range	Resolution	Accuracy
horizontal solar irradiation (W/m^2)	thermopile	0-2000 W/m^2	1 W/m^2	2nd class pyranometer
wind speed (m/s)	ultrasonic	0-60 m/s	0.01 m/s	whichever is greater 0.3 m/s or +/- 2% (0-35 m/s); +/- 3% (>35 m/s)
wind direction (°)	ultrasonic	0-360°	0.1°	+/-2% RMSE from 1.0 m/s
Relative humidity (%)	capacitive sensor	0-100% RH	0.1%	@ T= +15°C - +35°C: +/-1.5% (0-90%RH) +/- 2% RH (remaining field) @ T= -40°C - +15°C and +35°C - +60°C: +/- (1.5 + 1.5% of the measure)%RH
air temperature (°C)	PT100	-40°C - +60°C	0.1°C	+/- 0.15°C +/- 0.1 % of the measure
barometric pressure (hPa)	piezoresistive	600-1100 hPa	0.1 hPa	+/- 0.5 hPa @ 20 °C

The weather station generates data output every 10 seconds, based on measurements every 1 second. The data is sent through a FTP server to the website *www.wvmmonitor.eu*, where the information is stored in .cvs files and freely accessible. The weather station has a time deficiency of approximately 1.5 minute per year. The internal clock is checked and corrected, if necessary, monthly.

The air- and surface-monitoring installation generates data output every 10 seconds, based on measurements every 1 second. The data is collected through a WAGO datalogger, and sent through a FTP server to the website *www.wvmmonitor.eu*, where the information is stored in .cvs files and freely accessible. The internal clock is checked and corrected, if necessary, monthly.

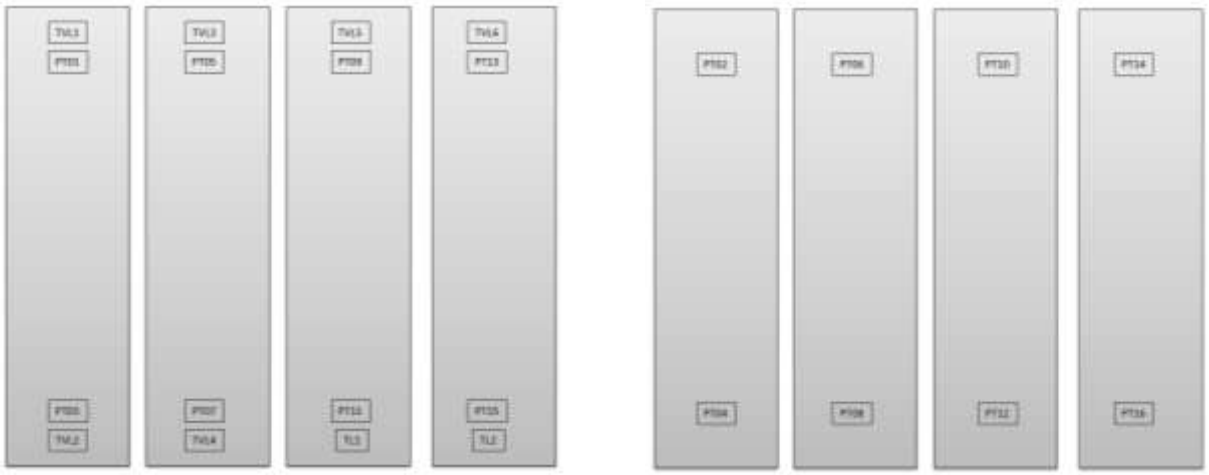

Fig. 8. and 9. Overview of monitoring sensors on the rooftop and on the PV segments in the field test. Abbreviations of sensors: TVL= air temperature, air velocity and relative humidity, PT=surface temperature, TL= air temperature and relative humidity.

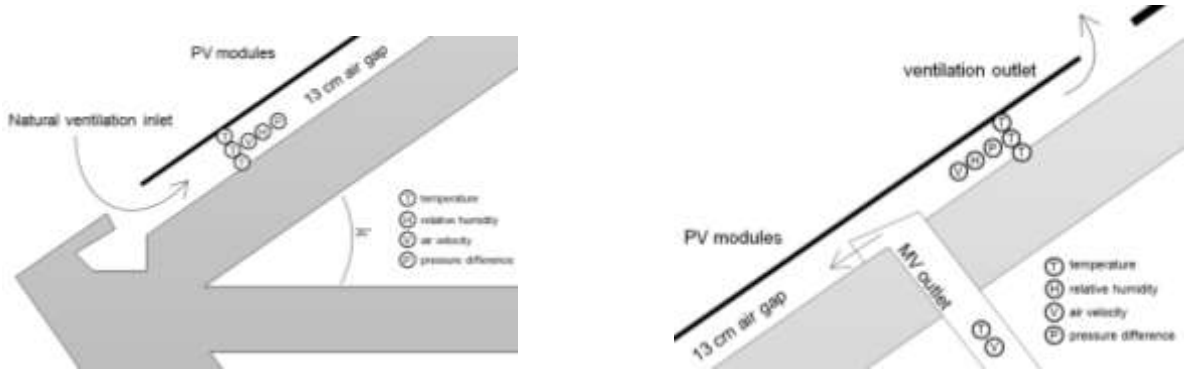

Fig. 10. and 11. Vertical sections of the bottom and top of the PV segments 1 and 2 with the locations of the different sensors, the realized air gap of 13 cm for back-string ventilation and the mechanical ventilation (MV) outlet.

The 6000 Wp BIPV system consisting of four segments with different quantities of back-string ventilation was installed in The District of Tomorrow (TDoT) in September 2011 and began its operation in December 2012. In December 2012, all monitoring equipment was installed and was connected to a web-based data logging system in May 2013. Data for PV output is generated in 5-minute intervals, based on measurements per second; all other data output is generated in 10- second intervals, based on measurements per second. The program MS Access and MS excel were applied to generate insight into the data collection presented in this research. The performance of the installation is monitored continuously since May 2013.

3 Preliminary results

In this section, the performance data of the installation is presented of three days in the different seasons spring, summer and fall, in the first year of monitored operation. This chapter consists of the measurements of the weather station, the PV output, and temperature sensors.

3.1 Selection of days

The following selected dates are based on the outside circumstances solar irradiation and temperature; the 28th of May, the 25th of July and the 11th of November 2013. The 28th of May was a partly cloudy spring day in the Netherlands, relatively cool in the morning with increasing temperatures during the day. In the afternoon there was some precipitation. Sunrise was at 4:31 and sundown at 20:36 summertime. The 16th of August was a mainly sunny summer day, with relative high Dutch summer temperatures. Sunrise was at 5:25 and sundown at 19:55 summertime. The 11th of November 2013 was a relatively mild partly cloudy autumn day. Sunrise was at 7:45 and sundown at 16:54 wintertime. Graphs 1 and 2 show the outside air temperature and solar irradiation on the selected days.

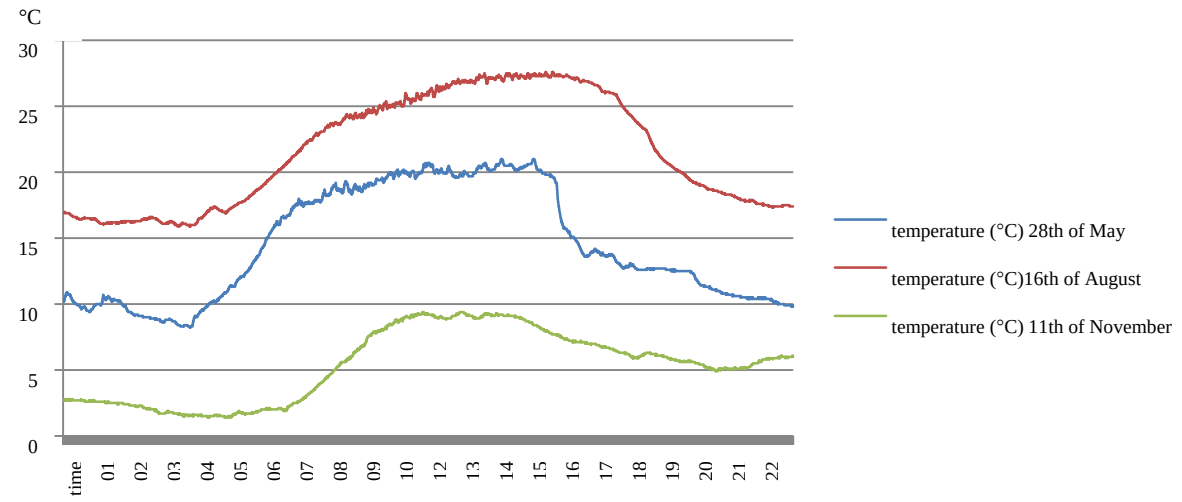

Graph 1. Outside air temperatures of the selected dates in this study at the location of the field test in The District of Tomorrow.

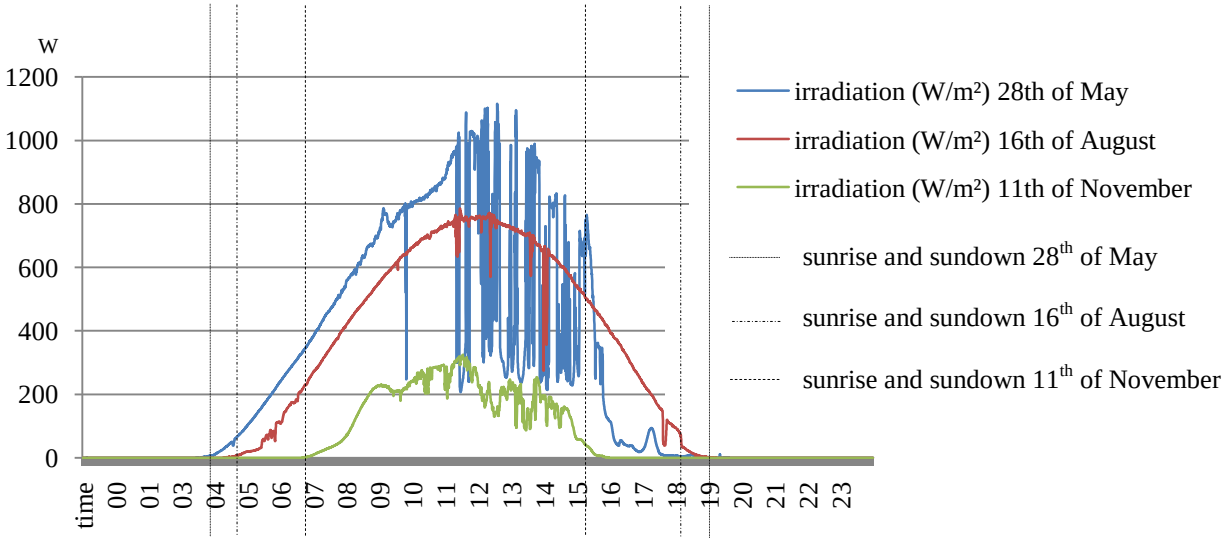

Graph 2. Solar irradiation and indication of sunrise and sundown on the selected dates in this study at the location of the field test in The District of Tomorrow.

Table 2 shows the total PV output per segment on the selected dates. Segment 4, the non-ventilated segment, shows a significantly lower output compared to the other three, ventilated, segments. In the following section PV output, temperature measurements and relative humidity are presented per day.

Table 2. Total output per segment (kWh) on the different selected dates.

Segment number	Total output (kWh) 28th of May	Total output (kWh) 16th of August	Total output (kWh) 11th of November
1	6.6	7.1	4.2
2	6.6	7.2	4.2
3	6.6	7.1	4.2
4	6.0	5.3	2.9

3.2 Results 28th of May 2013

In this section the PV output and surface temperatures are presented of the 28th of May 2013. In Graph 3 an overview is given of the PV output per segment in (W). The results show a comparable output for segments 1, 2 and 3. Graph 4 indicates the difference in electricity output (W) of segments 1, 2, and 4 compared to the naturally ventilated segment 3. Segment 4 shows a significantly lower output over the measurement period of 10%. Segments 1 and 2 show a similar output to segment 3.

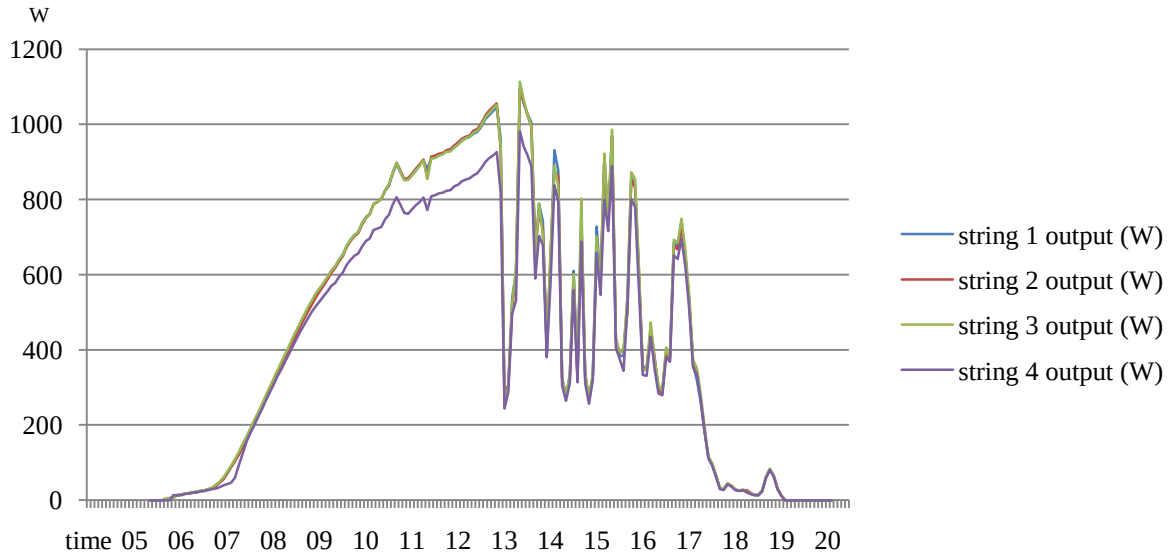

Graph 3. PV output (W) per segment on the 28th of May 2013 between sunrise and sundown.

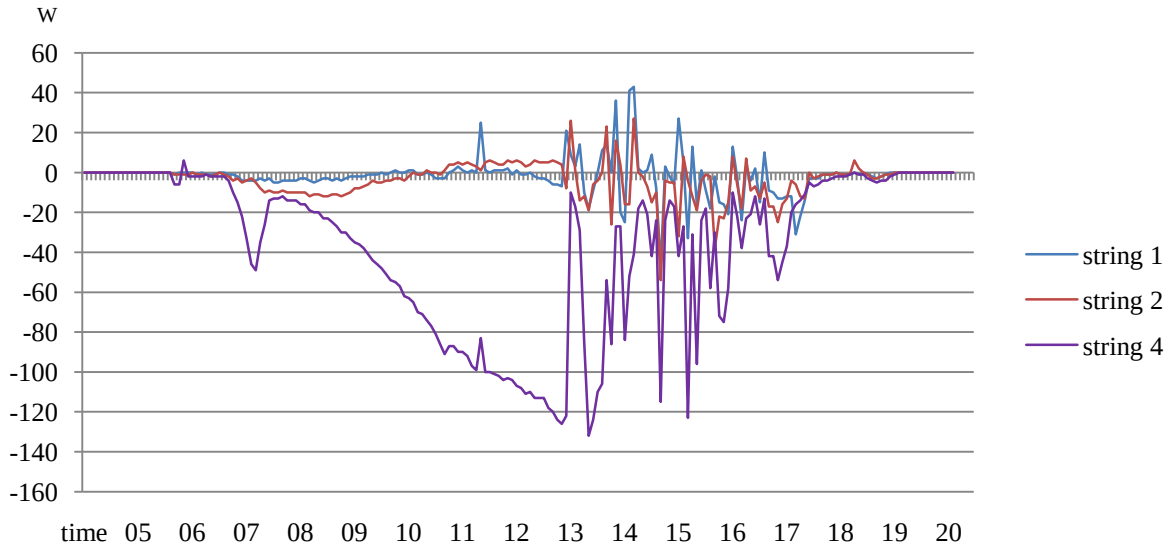

Graph 4. PV output (W) difference per segment compared with segment 3 on the 28th of May 2013 between sunrise and sundown.

Graph 5 shows an overview of average PV surface temperatures per segment (top and bottom). Average segment temperatures rise to above 60°C, while the temperature sensor on the PV segment number 4 indicates temperatures reaching 70°C on this moderately warm spring day in the Netherlands, with a maximum of 23°C outside air temperature. Between the segment averages, a difference of approximately 6°C is shown, while independent sensors indicate a difference of 35°C.

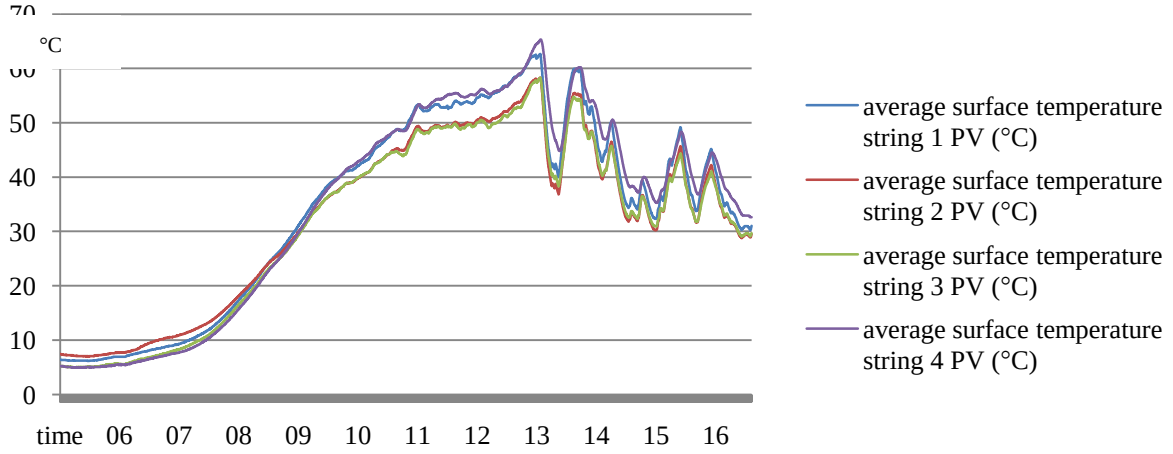

Graph 5. Average PV surface temperatures (°C) on the 28th of May 2013.

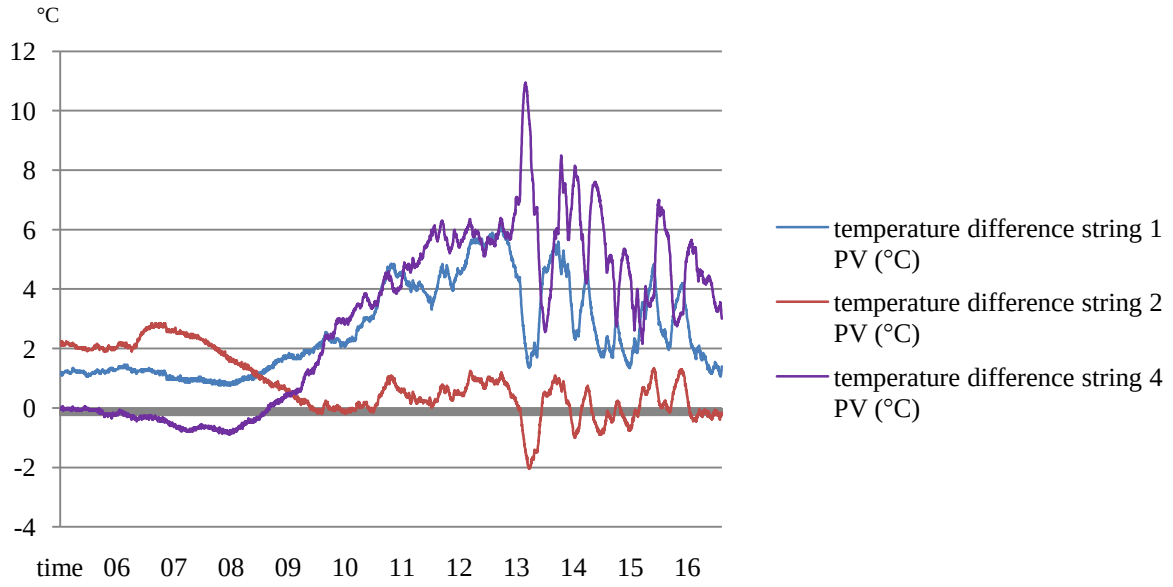

Graph 6 Average PV surface temperature differences (°C) between segments 1,2 and 4 compared with segment 3 on the 28th of May 2013.

3.3 Results 16th of August 2013

In this section the PV output and surface temperatures are presented of the 16th of August 2013. In Graph 7 an overview is given of the PV output per segment in (W). The results show a comparable output for segments 1, 2 and 3. Graph 8 indicates the difference in electricity output (W) of segments 1, 2, and 4 compared to the naturally ventilated segment 3. Segment 4 shows a significantly lower output over the measurement period of over 30%. Segment 1 and 2 show a higher power output (1 % to 4%).

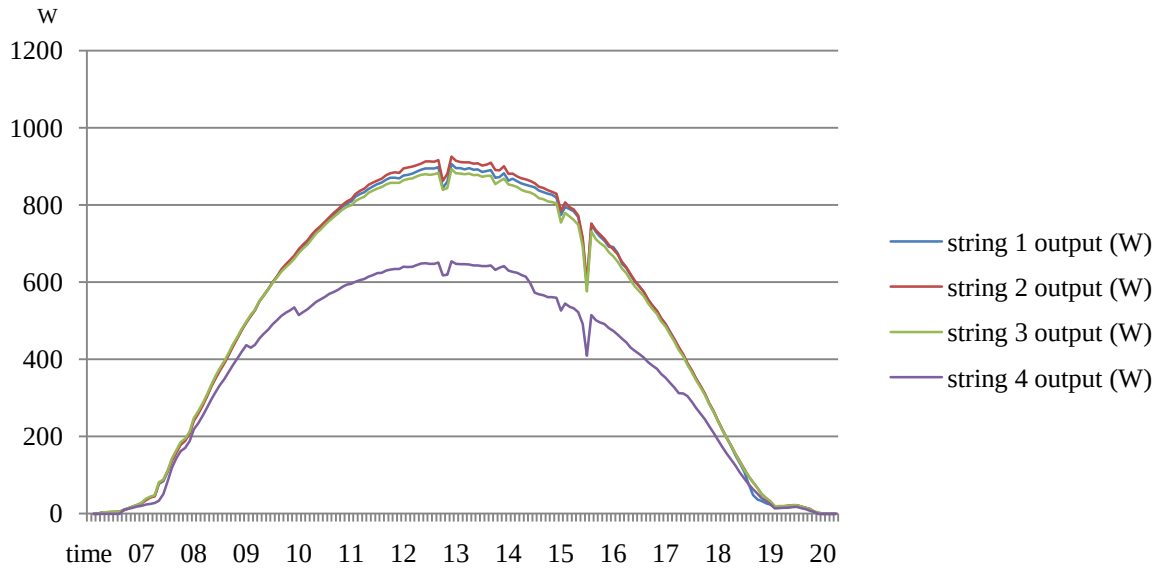

Graph 7. PV output (W) per segment on the 16th of August 2013 between sunrise and sundown.

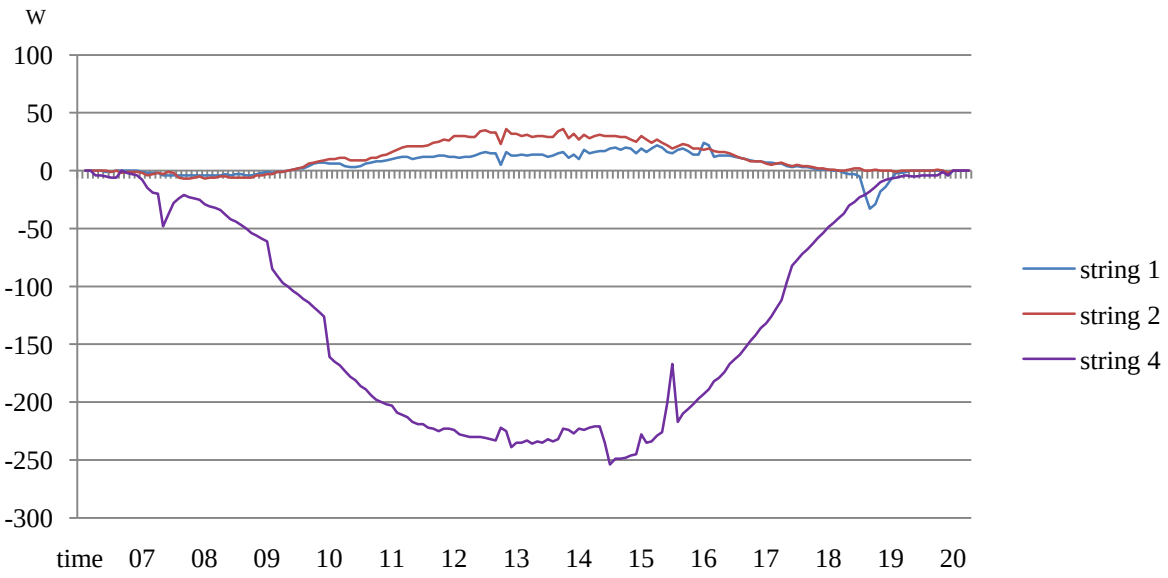

Graph 8. PV output (W) difference per segment compared with segment 3 on the 16th of August 2013 between sunrise and sundown.

Graph 9 shows an overview of average PV surface temperatures per segment (top and bottom). Average segment temperatures rise to above 60°C, while temperature sensor on the PV segment number 4 indicate temperatures reaching 70°C, with a maximum 28°C outside air temperature. Between the segment averages a difference of approximately 11°C is shown, while independent sensors indicate a difference of 30°C.

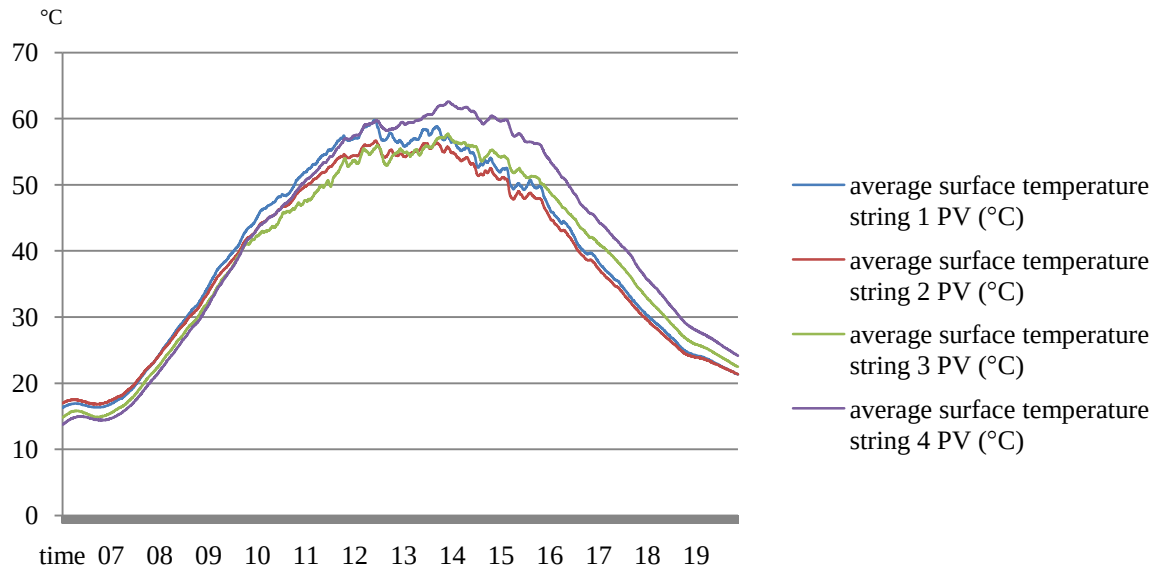

Graph 9. Average PV surface temperatures(°C) on the 16th of August 2013.

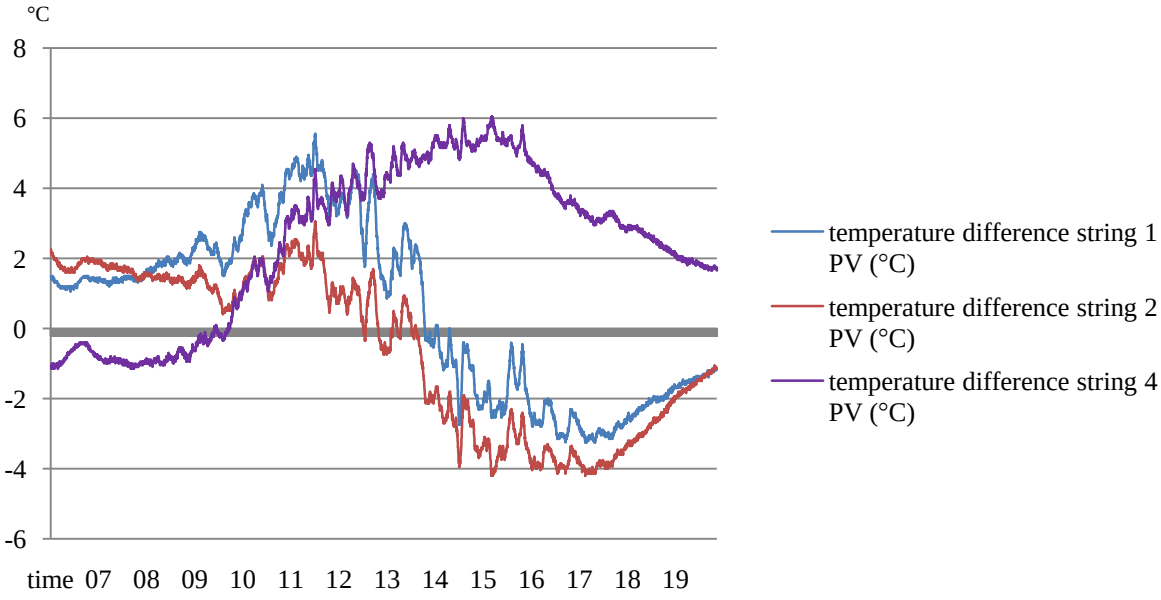

Graph 10. Average PV surface temperature differences (°C) between segments 1,2 and 4 compared with segment 3 on the 16th of August 2013.

3.4 Results 11th of November 2013

In this section the PV output and surface temperatures are presented of the 11th of November 2013. In Graph 11 an overview is given of the PV output per segment in (W). The results show a comparable output for segments 1, 2 and 3. Graph 12 indicates the difference in electricity output (W) of segments 1, 2, and 4 compared to the naturally ventilated segment 3. Segment 4 shows a significantly lower output over the measurement period of over 40%. Due to the fluctuation of solar irradiation differences between the different segments 1,2 and 3 are negligible on the total output on this day (4.2 kWh per segment).

W

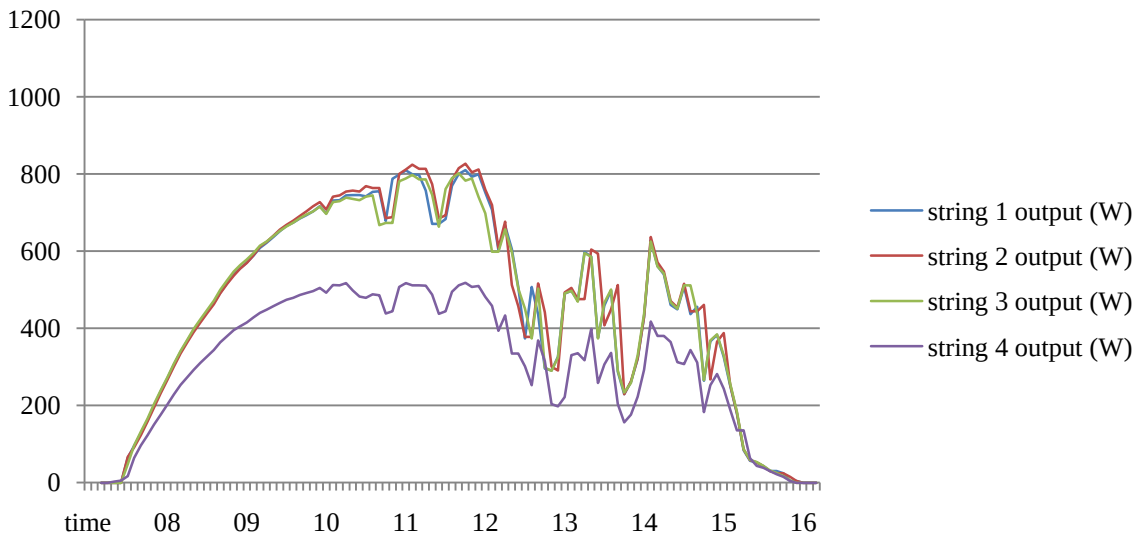

Graph 11. PV output (W) per segment on the 11th of November 2013 between sunrise and sundown.

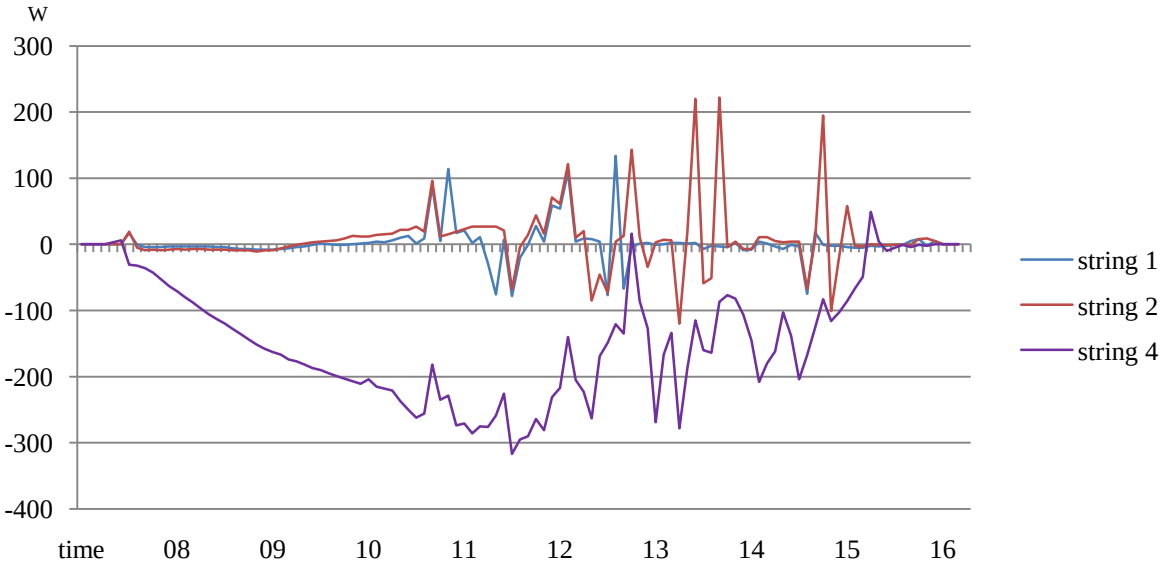

Graph 12. PV output (W) difference per segment compared with segment 3 on the 16th of August 2013 between sunrise and sundown.

Graph 13 shows an overview of average PV surface temperatures per segment (top and bottom). Average segment temperatures rise to above 35°C, while the temperature sensor on the PV segment number 4 indicate temperatures reaching 45°C on this moderate sunny autumn day in the Netherlands, with a maximum 9°C outside air temperature. Between the segment averages a difference of approximately 5°C is shown, while independent sensors indicate a difference of 23°C is.

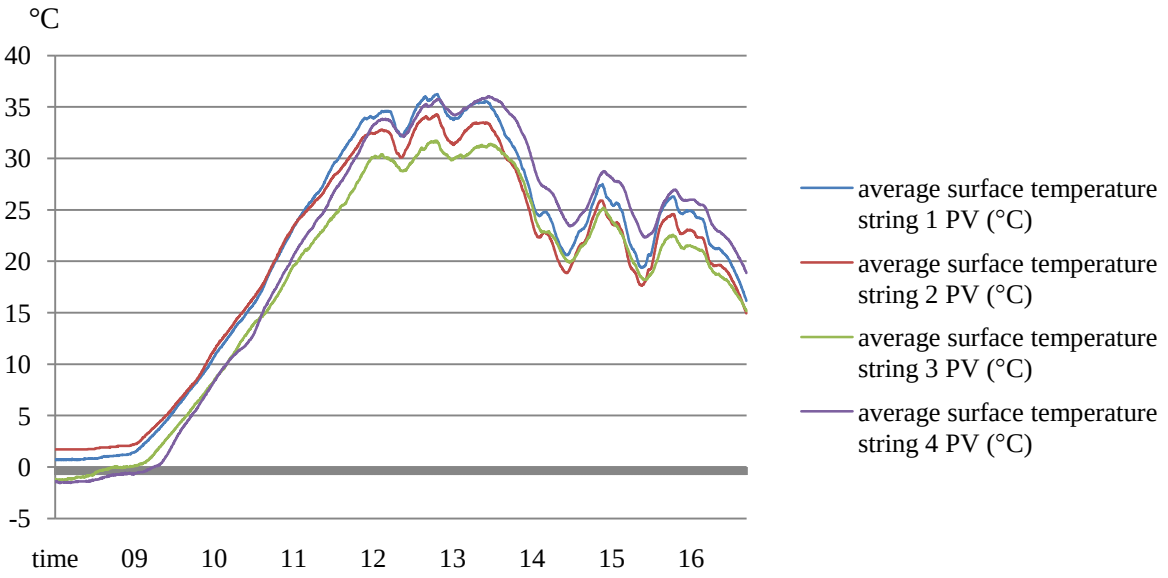

Graph 13. Average PV surface temperatures(°C) on the 11th of November 2013.

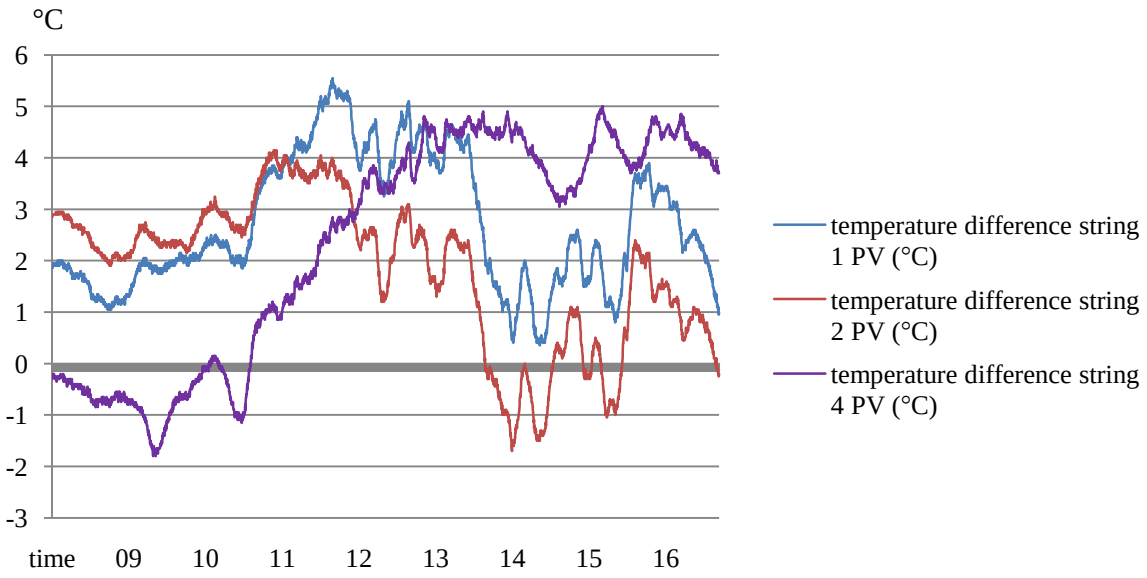

Graph 14. Average PV surface temperature differences (°C) between segments 1,2 and 4 compared with segment 3 on the 11th of November 2013.

4 Conclusions and discussion

This first analysis of a selection of data collected in the BIPV field test in The District of Tomorrow in the Netherlands indicates that ventilation might prove to be an effective way to prevent PV panels from accumulating heat with collateral negative effects on PV output and lifespan. The results indicate that temperature differences of individual sensors vary between 23°C on an autumn day and 35°C on a spring day. PV output differences vary between 10% on a spring day and over 40% on an autumn day. Theoretically, with 0.5% PV output decrease, a difference of 17.5% on a spring day and 10% on an autumn day would be expected. Outside circumstances such as solar irradiation, wind and temperature have been left out of this first study, but will be investigated to indicate more clearly the relation between back-string ventilation and PV output. The decreased efficiency of the PV modules throughout time might indicate that the increased temperatures in the non-ventilated segment have a negative effect on the lifespan of the PV modules.

Based on this study of three days, an indication has been given for the temperature developments in BIPV solutions in the Netherlands. Long-term data evaluation is necessary and will be conducted to generate insight into the long-term effect of back-string ventilation on BIPV efficiency.

5 Acknowledgement

This study is part of the research projects IMDEP conducted by Zuyd University of Applied Sciences together with knowledge and industrial partners in the research infrastructure of The District of Tomorrow. The authors would like to thank the Dutch Organization for Scientific Research NWO for partly funding this research.

6 References

[1] (IEA), I.E.A., *Worldwide trends in energy use and efficiency*. 2008.

[2] Ko, J. and L. Widder. *building envelope assessment tool for system integrated design*. in *PLEA 2011*. 2011. Louvain-la-Neuve, Belgium.

[3] Pérez-Lombard, L., J. Ortiz, and C. Pout, *A review on buildings energy consumption information.* Energy and Buildings, 2008. **40**(3): p. 394-398.

[4] (USEIA), U.S.E.I.A., *International Energy Outlook 2011*. 2011, U.S. Energy Information Administration.

[5] Bruckner, M., et al., *Materials embodied in international trade – Global material extraction and consumption between 1995 and 2005.* Global Environmental Change, 2012. **22**(3): p. 568–576.

[6] Frontini, F. *daylight and solar control in building: a new angle selective see-thorough PV-facade for solar control*. in *PLEA 2011*. 2011.

[7] Torcellini, P., et al., *Zero Energy Buildings: A Critical Look at the Definition*, in *ACEEE Summer Study*. 2006, NREL: California.

[8] AgentschapNL, *Nationaal Plan voor het bevorderen van bijna-energieneutrale gebouwen in Nederland*. 2012.

[9] Ho, C.J., A.O. Tanuwijava, and C.-M. Lai, *Thermal and electrical performance of a BIPV integrated with a microencapsulated phase change material layer.* Energy and Buildings, 2012. **50**(0): p. 331-338.

[10] Chynoweth, P. *The built environment interdiscipline: a theoretical model for decision makers in research and teaching*. Structural Survey [conceptual paper] 2009 2009 [cited 27 4]; 301-310].

[11] Mekhilef, S., R. Saidur, and M. Kamalisarvestani, *Effect of dust, humidity and air velocity on efficiency of photovoltaic cells.* Renewable and Sustainable Energy Reviews, 2012. **16**(5): p. 2920-2925.

[12] Davis, M.W., B. dougherty, and A. Fanney, *Prediction of building integrated photovoltaic cell temperatures.* the Journal of Solar Energy Engineering, 2001. **123**(2): p. 200-210.

[13] Sadineni, S.B., S. Madala, and R.F. Boehm, *Passive building energy savings: A review of building envelope components.* Renewable and Sustainable Energy Reviews, 2011. **15**(8): p. 3617-3631.

[14] Bloem, J.J., et al., *An outdoor Test Reference Environment for double skin applications of Building Integrated PhotoVoltaic Systems.* Energy and Buildings, 2012. **50**(0): p. 63-73.

[15] Huang, M.J. *two phase change materials with different closed shape fins in building integrated photovoltaic system temperature regulation*. in *World Renewable Energy Congress 2011*. 2011. Linkoping, Sweden.

[16] Maturi, L., et al. *analysis and monitoring results of a BIPV system in northern Italy*. in *PVSEC*. 2010. Valencia, Spain.

[17] Petter Jelle, B., C. Breivik, and H. Drolsum Røkenes, *Building integrated photovoltaic products: A state-of-the-art review and future research opportunities.* Solar Energy Materials and Solar Cells, 2012. **100**(0): p. 69-96.

[18] Tyagi, V.V., S.C. Kaushik, and S.K. Tyagi, *Advancement in solar photovoltaic/thermal (PV/T) hybrid collector technology.* Renewable and Sustainable Energy Reviews, 2012. **16**(3): p. 1383-1398.

[19] Gan, G., *Numerical determination of adequate air gaps for building-integrated photovoltaics.* Solar Energy, 2009. **83**(8): p. 1253-1273.

[20] Wang, Y., et al., *Influence of a building's integrated-photovoltaics on heating and cooling loads.* Applied Energy, 2006. **83**(9): p. 989-1003.

[21] Norton, B., et al., *Enhancing the performance of building integrated photovoltaics.* Solar Energy, 2011. **85**(8): p. 1629-1664.

[22] Gan, G., *Effect of air gap on the performance of building-integrated photovoltaics.* Energy, 2009. **34**(7): p. 913-921.

[23] Mei, L., et al., *Equilibrium thermal characteristics of a building integrated photovoltaic tiled roof.* Solar Energy, 2009. **83**(10): p. 1893-1901.

[24] Hasan, A., et al., *Evaluation of phase change materials for thermal regulation enhancement of building integrated photovoltaics.* Solar Energy, 2010. **84**(9): p. 1601-1612.

[25] Quesada, G., et al., *A comprehensive review of solar facades. Opaque solar facades.* Renewable and Sustainable Energy Reviews, 2012. **16**(5): p. 2820-2832.

[26] NREL, N.R.E.L., *procedure for measuring and reporting the perfomance of photovoltaic systems in buildings*. 2005.

[27] (IEC), I.E.C., *IEC 61724 International standard photovoltaic system performance monitoring - guidelines for measurement, data exchange and analysis* 1998, IEC.

[28] Pacheco, R., J. Ordóñez, and G. Martínez, *Energy efficient design of building: A review.* Renewable and Sustainable Energy Reviews, 2012. **16**(6): p. 3559-3573.

[29] Bahaj, A.S., *Photovoltaic roofing: issues of design and integration into buildings.* Renewable Energy, 2003. **28**(14): p. 2195-2204.

[30] De Lillo, A., et al. *effects of BIPV on performance*. in *PV SEC*. 2004. Paris, France.

[31] Sanjuan, C., et al., *Energy performance of an open-joint ventilated façade compared with a conventional sealed cavity façade.* Solar Energy, 2011. **85**(9): p. 1851-1863.

[32] Fujisawa, T. and T. Tani, *Annual exergy evaluation on photovoltaic-thermal hybrid collector.* Solar Energy Materials and Solar Cells, 1997. **47**(1–4): p. 135-148.

[33] Ghani, F., M. Duke, and J.K. Carson, *Effect of flow distribution on the photovoltaic performance of a building integrated photovoltaic/thermal (BIPV/T) collector.* Solar Energy, 2012. **86**(5): p. 1518-1530.

[34] Omer, S.A., R. Wilson, and S.B. Riffat, *Monitoring results of two examples of building integrated PV (BIPV) systems in the UK.* Renewable Energy, 2003. **28**(9): p. 1387-1399.

[35] Yun, G.Y., M. McEvoy, and K. Steemers, *Design and overall energy performance of a ventilated photovoltaic façade.* Solar Energy, 2007. **81**(3): p. 383-394.
[36] Kaan, H. and T. Reijenga, *photovoltaics in an architectural context.* progress in photovoltaics: research and applications, 2004. **12**: p. 395-408.
[37] KNMI. *Maastricht, langjarig gemiddelden, tijdvak 1981-2010*. 2013; Available from: *http://www.klimaatatlas.nl/tabel/stationsdata/klimtab_8110_380.pdf*.
[38] (IEC), I.e.c., *IEC 1829 Chrystalline silicon photovoltaic (PV) array - on-site measurement of I-V characteristics*. 1995.